JPE 17-5-20

https://doi.org/10.6113/JPE.2017.17.5.1327
ISSN(Print): 1598-2092 / ISSN(Online): 2093-4718

Enhanced Simulated Annealing-based Global MPPT for Different PV Systems in Mismatched Conditions

Feng Wang†, Tianhua Zhu*, Fang Zhuo*, Hao Yi*, and Yusen Fan*

†,*State Key Laboratory of Electrical Insulation and Power Equipment, Xi'an Jiaotong University, Xi'an, China

Abstract

Photovoltaic (PV) systems are influenced by disproportionate impacts on energy production caused by frequent mismatch cases. The occurrence of multiple maximum power points (MPPs) adds complexity to the tracking process in various PV systems. However, current maximum-power point tracking (MPPT) techniques exhibit limited performance. This paper introduces an enhanced simulated annealing (ESA)-based GMPPT technique against multiple MPP issues in P–V curve with different PV system structures. The proposed technique not only distinguishes global and local MPPs but also performs rapid convergence speed and high tracking accuracy of irradiance changing and restart capability detection. Moreover, the proposed global maximum power tracking algorithm can be applied in the central converter of DMPPT and hybrid PV system to meet various application scenarios. Its effectiveness is verified by simulation and test results.

Key words: Distributed MPPT, GMPPT, Mismatch, PV generation, Simulated annealing

I. INTRODUCTION

Mismatching is an unavoidable situation that significantly affects the power generation capability of a photovoltaic (PV) system. Generally, PV units are in a series and parallel connection to meet certain power rating and bus voltage requirements. For traditional centralized and string-level maximum power point tracking (MPPT) PV systems in mismatch cases, not all PV units can operate at their respective maximum power points (MPPs) because they are coupled according to the connection structure. Parallel PV units are forced to operate at the same terminal voltage. Similarly, the PV units are forced to work at the same string current in a series connection. When the shaded panels in a series connection cannot generate enough current, their bypassed diodes conduct to protect the panels from hotspot effect and introduce multiple MPPs on the P–V output curves. Traditional MPPT algorithms are designed to only address uniform insolation and cannot adequately consider the abovementioned mismatch cases. Consequently, the development of advanced global MPPT (GMPPT) techniques is suitable for its application in different mismatch conditions in real-world cases is critical. The appearance of multiple MPPs not only results in malfunction but also degrades the output power of the traditional MPPT algorithm. Moreover, multiple peak appearances can mislead traditional MPPT algorithms to be trapped at local peaks [1]-[3].

Mostly, techniques that are suitable for the mismatch in the current literature can be divided into firmware-based solutions and hardware architecture-based solutions [4]. As a typical hardware architecture-based solution, distributed MPPT (DMPPT) concept has been introduced in [5], [6]. This solution can minimize the effect of mismatch from panel level and the following pros and cons are summarized in [3], [7], [8]:

1) DMPPT effectively strengthens the capability to resist mismatch threats and improve power generation performance.

2) Enlarged optimal power region (OPR) and easy MPPT realization of the central inverter are obtained.

3) Flexible and reliable design is achieved.

4) Improved performance is ensured in data acquisition and management, particularly in unexpected fire and other emergencies.

However, even the DMPPT solution is not always effective in making each PV unit work on its MPP, especially in heavy mismatch [9]. The limited voltage gain of the adopted converter circuit and the finite power ratings of devices result in the mismatched power loss in the PV system, even when it is

Manuscript received Mar. 21, 2017; accepted Jun. 20, 2017
Recommended for publication by Associate Editor Jong-Bok Baek.
†Corresponding Author: fengwangee@xjtu.edu.cn
Tel: +86-15829389307, Xi'an Jiaotong University
*State Key Laboratory of Electrical Insulation and Power Equipment, Xi'an Jiaotong University, China

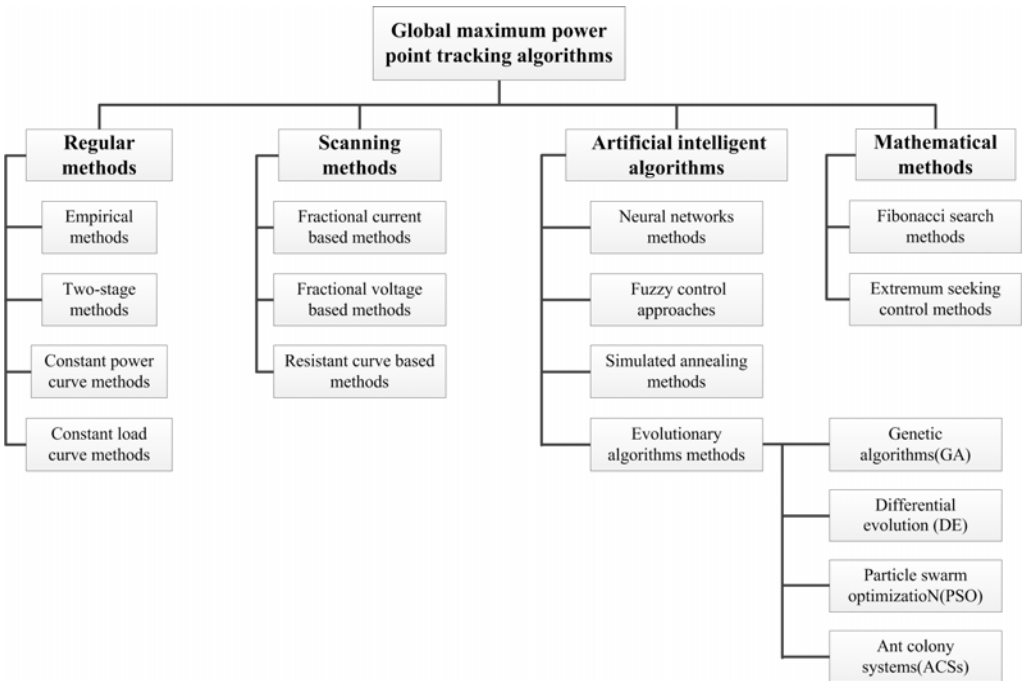

Fig. 1. Classification of GMPPT methods.

equipped with DMPPT converters. Joint adoption of DMPPT and central MPPT is approved to be necessary in the DMPPT system, and the synergetic control is also proven to be required [7], [10], [11]. For the second central MPPT control in the DMPPT system, the multi-peak issue and challenging central MPPT strategy still exist.

To address the aforementioned multiple MPP issues under mismatch cases, a number of GMPPT methods have been explored, as shown in Fig. 1 [12]-[20]. Two-stage GMPPT method was proposed in [21]. In this method, the first stage is used to search for the GMPP location interval of the multi-peak P–V curve. The second stage introduces traditional MPPT methods to search for the precise GMPP location. The tracking speed of this method is fast because the first stage only requires one step to move the operating point to the vicinity of the GMPP. The tracking time of this method is similar to that of traditional MPPT methods. However, disadvantages also exist. First, the open-circuit voltage and the short circuit current of the system are required, resulting in high power loss during the detection process. Second, the length of the interval is difficult to determine in various PV systems and mismatch conditions. Unlike the two-stage method, Fibonacci MPPT is based on mathematical theories in which GMPP is solved by gradually reducing the search range [22], [23]. In the PSO method, each particle is defined by its own position and velocity. The performance of the method is highly influenced by the experiences of neighboring particles. Each particle follows the current best-performing particle to search within the solution space. PSO can conduct GMPPT in distributed and centralized architecture because it is an optimization method based on swarming. The PSO-based GMPPT method is based on the flocking and schooling behavior of birds and fishes, respectively. The particles solve a problem by sharing their individual information to all of the particles. However, random variables limit the performance in its implementation. Moreover, a large number of parameter definitions for each system is required [17], [20]. In papers [15] and [16], simulated annealing (SA)-based GMPPT method has been introduced in the area of GMPPT control. Compared with the widely used Perturb and Observe (P&O) method, this algorithm can track the GMPP with a certain probability without increasing the complexity. Moreover, the SA-based algorithm depends strictly on system parameters and is independent of the initial settings of the system. All aforementioned features prove that SA is a promising and effective method for GMPPT application. In fact, the proposal of a fair benchmark for various techniques mentioned in the literature is difficult, primarily because various PV generation systems (including power rating and power converter topology) and shading patterns are considered to verify the effectiveness of the algorithms. The performances of the six typical GMPPT algorithms are selected and compared based on features such as complexity, efficiency, speed, oscillation, dependence on system parameters, stability, and economics, as shown in Table I [27], [28].

This paper presents an enhanced SA (ESA)-based GMPPT technique to perform better power generation in mismatch cases. Compared with traditional SA-based solutions, the proposed technique improves the MPPT performance under changing irradiance cases, optimizing the existing strategies on GMPP tracking accuracy, convergence speed in tracking process, and self-restarting and power generation capabilities in

TABLE I
COMPARISON OF DIFFERENT GMPPT METHODS

	Empirical method	Two-step method	Fractional current-based method	Fibonacci method	PSO-based method	SA-based method
Complexity	easy	easy	normal	complex	normal	normal
Efficiency	high	high	low	high	high	high
Speed	fast	fast	fast	slow	slow	fast
Oscillation	yes	yes	no	no	no	no
Dependence on system parameters	high	low	low	low	low	low
Stability	high	high	high	low	low	high
Cost	low	low	high	low	low	low

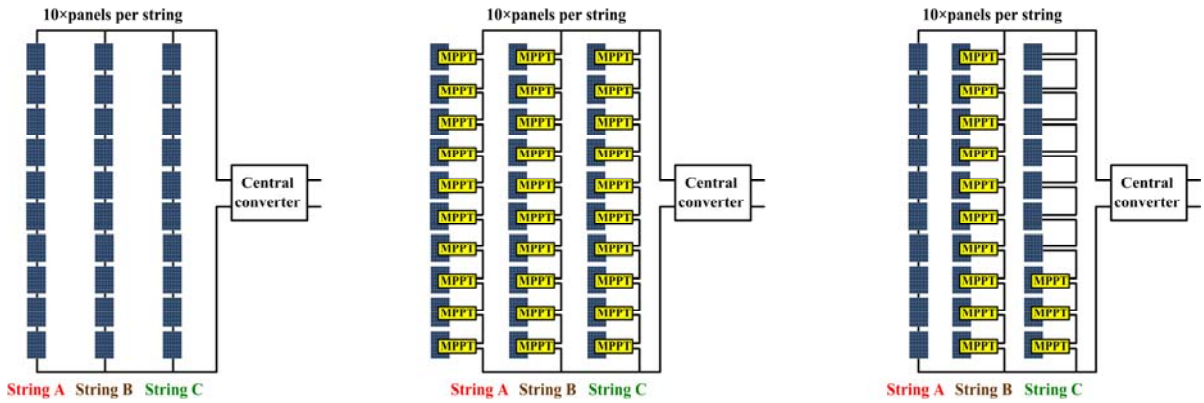

(a) Original PV array. (b) DMPPT array. (c) Hybrid PV array.
Fig. 2. Different structure of PV array.

rapid changing irradiance. The proposed ESA-based MPPT algorithm can achieve the GMPP of the original PV, DMPPT PV, and hybrid PV systems. The rest of this paper is organized as follows. Section II presents the static analysis and output characteristic curves of the original PV array, DMPPT PV system, and hybrid PV system in mismatch cases. Section III presents the working principle and advantages of an ESA-based GMPPT. Section IV provides a comparison between the simulation and experimental results to validate the proposed ESA-based GMPPT algorithm. Section V draws the conclusions.

II. OUTPUT CURVE OF DIFFERENT PV SYSTEMS UNDER MISMATCH CASES

Mostly, PV panels are connected in series and/or parallel according to the requirements of bus voltage and power rating, as shown in Fig. 2(a). To improve the power generation ability in mismatch, the DMPPT concept is introduced in this PV array, and is referred as the "module integrated converter (MIC)." The adoption of MIC achieves greater flexibility of design than the traditional PV array. Typically, a DMPPT PV system is used to equip all of the PV panels with a MPPT converter, as shown in Fig. 2(b). This structure is optimized for mismatches between panels and between strings to maximize the system power generation efficiency by re-capturing the energy that would have been lost because of the mismatch. This decoupled construction can effectively solve mismatch issues. However, the installation and later maintenance of this structure are costly.

In most cases, the PV array suffers a mismatch case with certain panels at fixed positions, such as the shading of surrounding trees and overhead power lines. To achieve the optimal state of the system, tradeoff should be made between the cost and anti-mismatch capabilities. The hybrid PV array is proposed to partially apply DMPPT converters in the installation of a PV array, which is shown as Fig. 2(c). This configuration can eliminate mismatch at fixed position and maximize the array power output with less cost.

A case study is introduced to conceptualize the output characteristic of aforementioned PV systems. The P–V curve of string C in the original PV array is obtained, which is shown as a green dashed curve in Fig. 3(a). The P–V curve of this PV string has a multi-peak characteristic, which makes the traditional MPPT algorithm more difficult.

The performance of the PV string C is improved after the adoption of DMPPT converters. Fig. 3(b) shows that the introduction of DMPPT converters not only eliminates the multi-peak issue but also presents an optimal power region, which can operate all PV units that operate on its MPP regardless of irradiance levels [10], [11], [24], [25]. If a part of the PV panels in string C are equipped with MICs, then the output P–V curve of hybrid string C can be recovered but still cannot achieve an ideal maximum power in partial mismatch

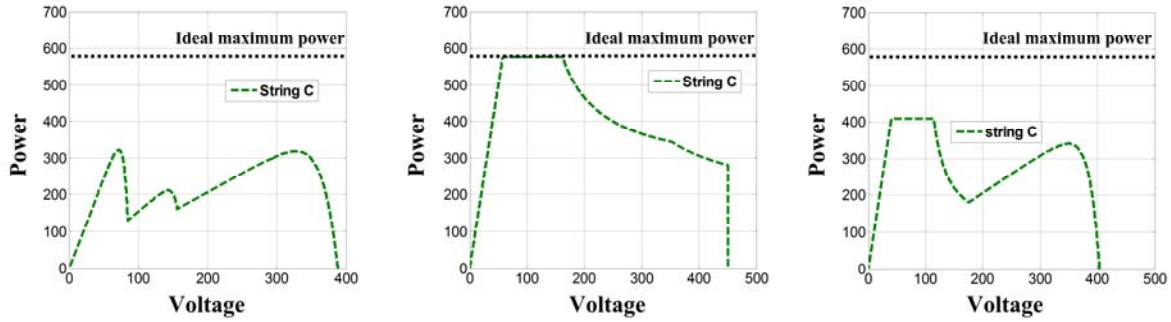

(a) Original PV string C. (b) DMPPT string C. (c) Hybrid string C.

Fig. 3. Output curves of string C.

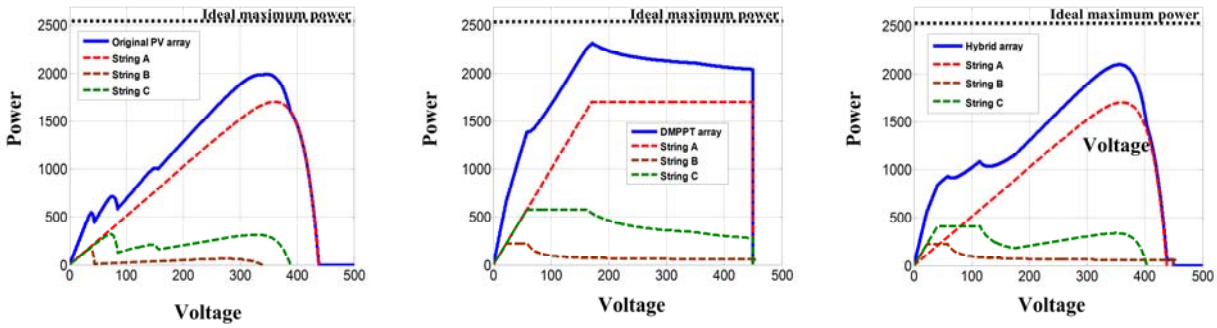

(a) Original PV array. (b) DMPPT PV array. (c) Hybrid PV array.

Fig. 4. Output curves of PV systems in heavy mismatch case.

power cases, as shown in Fig. 3(c).

Fig. 4(a)-(c) show the output curves to further analyze the PV string and PV array. The power generation capability in this heavy mismatch case increases along with the adoption rate of MICs. However, in this case, even the P–V curve of the DMPPT system cannot achieve the ideal maximum power, and the multi-peak characteristic issue remains, which is challenging for the second central MPPT control.

In summary:

1) The adoption of DMPPT solution effectively strengthens the capability to resist mismatch and improves the power generation performance.

2) Even when DMPPT converters are equipped with all PV panels in the system, obtaining an ideal maximum power in a severe mismatch case is still not guaranteed.

3) The cooperative control of the DMPPT control and the centralized MPPT control are needed even in the DMPPT system.

4) A flexible and reliable GMPPT algorithm is essential for the original PV system, DMPPT system, and hybrid PV system to fundamentally address the mismatch issue.

III. Operation Principle of Proposed ESA-based GMPPT Algorithm

To track the GMPP in different mismatch cases, the SA concept is adopted and applied in PV generation [12]. This algorithm can avoid being trapped in local MPPs by accepting operating points of lower power ratings. This algorithm does not need the specific characteristics of the P–V curve or the initial parameters of the shaded PV system, which presents inherent superiority over existing GMPPT algorithms.

However, the SA algorithm is suitable for tracking the maxima on a static curve but cannot tackle irradiance changes. The number of iterations is determined only by system parameters (i.e., initial temperature, cooling rate, and final temperature), which either degrade the tracking accuracy or slow down the tracking speed. Worse still, the ill-defined (or undefined) neighborhood of the voltage perturbation results in significant power losses and long tracking time.

To address the aforementioned problems, three major improvements on restarting capability, stopping criterion, and self-adaptively adjustable neighborhood are introduced. This ESA-based GMPPT algorithm provides improved performance, such as robust with faster speed, less power losses, and higher tracking accuracy. By making the neighborhood of voltage perturbation self-adaptively adjustable, the ESA method performs with faster convergence speed and lower power losses. Refining the algorithm stopping criterion, we observe higher tracking accuracy. By adding a power-variation detection mechanism, we introduce a self-restarting capability to enable the algorithm to deal with irradiance changes.

A. Restarting Capability

When the GMPP of the PV system is reached, the ESA-based GMPPT algorithm stops perturbing the voltage and generates

fixed voltage reference V_{mpp}. At this moment, the power of the current operating point (Pi) is measured and stored. Subsequently, a power variation evaluation process is launched as follows:

$$\Delta P = \left| P_i - P_{max} \right|, \tag{1}$$

where P_{max} is the value of the GMPP acquired in the previous tracking operation, and the restarting criterion is

$$\frac{\Delta P}{P_{max}} > \delta, \tag{2}$$

where the ratio of ΔP to P_{max} is greater than a given threshold value. The algorithm recognizes that an environmental change has occurred and the tracking procedure should be restarted. This restarting capability enables the system to respond quickly under changing irradiance levels.

B. Advanced Stopping Criterion

The stopping criteria in the current SA method shows that the temperature T reaches the preset minimum temperature T_{min}, which signifies that the number of iterations is only determined by system parameters (i.e., initial temperature, cooling rate, and final temperature). Possibly, when the iterations end, the GMPP has not been tracked. Therefore, the tracking accuracy cannot be ensured. In the proposed ESA-based GMPPT method, an optimized stopping criterion is used to increase the tracking accuracy.

The definition of the parameter *flag* is defined to terminate the GMPP search of the ESA-based GMPPT algorithm.

If the inequality in (2) is not true, i.e.,

$$\frac{\Delta P}{P_{max}} < \delta, \tag{3}$$

then

$$flag = flag + 1. \tag{4}$$

When *flag* exceeds the constant *N*, the *N* successive working points output similar powers. Thus, the peak power is reliably reached and the MPPT accuracy is increased significantly.

C. Flexible Self-Adaptive Neighborhood

In the existing SA method, the voltage generation is completely random, thereby resulting in significant power loss and long tracking time. Therefore, in the proposed ESA-based GMPPT method, a self-adaptive, adjustable neighborhood is defined to optimize the tracking process.

If the number of accepted perturbations is greater than the rejected perturbations, then the perturbation step is relatively small. Therefore, an appropriate efficient neighborhood value has to be optimized to keep the number of acceptable and rejected perturbations almost equal. To further optimize the algorithm, a flexible, self-adaptive neighborhood definition is introduced in the following.

The output voltage of the PV system is perturbed N_S times under a fixed step. *No_accept* records the number of accepted points. After N_S perturbations, the algorithm adjusts the step to be more reasonable. If *No_accept*>0.6*N_S, i.e., over a half of the N_S perturbations are accepted, then the general trend of the perturbation is toward the MPP and the current step is relatively small. Therefore, the step should be regulated to a larger value to accelerate the tracking toward the MPP. If *No_accept*<0.4*N_S, i.e., less than half of the N_S perturbations are accepted, and then the perturbations may be out of the neighborhood of the MPP and the current step is relatively large. As a result, the step should be regulated to a smaller value to converge the tracking to the MPP; otherwise, the step remains constant. The tracking becomes more specific, the convergence speed becomes faster, and the power oscillation is reduced with the well-designed neighborhood.

$$\left.\begin{array}{ll} \text{new } step = step \times \left(1+2\times \dfrac{No\_accept / N_S - 0.6}{0.4} \right), & \text{if } No\_accept > 0.6\times N_S \\ \text{new } step = \dfrac{step}{1+2\times \dfrac{0.4 - No\_accept / N_S}{0.4}}, & \text{if } No\_accept < 0.4\times N_S \\ \text{new } step = step, & \text{else} \end{array}\right\} \tag{5}$$

The flowchart of the proposed ESA-based GMPPT control strategy is shown in Fig. 5. The process of the ESA-based GMPPT method is as follows:

1. Initialization of all parameters, including the temperature and the cooling rate value.
2. Selection of a random voltage V_i (0-V_{OC}).
3. Measurement of the corresponding power (P_i).
4. Repetition of the following steps until the stop criterion is satisfied:

a) Randomly select V_k. $V_k = V_i + r\times step$, where r is a random number between −1 and 1.

b) Calculate P_k. Meanwhile, increase the variable *No_perturb* by 1.

c) When $P_k > P_i$, V_k is set as the new reference voltage (i.e., $V_i = V_k$). If P_k is larger than P_{max}, then set $P_{max} = P_k$, $V_{max} = V_k$. Thus, *No_accept* is increased by 1.

d) Else, when $P_k < P_i$, the updated voltage point may still be accepted based on the set acceptance probability:

$$P_r = \exp\left[\frac{P_k - P_i}{T_k} \right]. \tag{6}$$

This probability has high correlation to the power difference and current temperature. P_k and P_i indicate current power and the previous power reference, respectively. T_k is the current temperature. Low temperature implies small possibility of accepting operating points with smaller power [12], [26]. If accepted, then *No_accept* is increased by 1.

e) When N_S perturbations have been operated under the step, regulate the step value, as shown in (5). Reset *No_perturb*, *No_accept*, and increase *No_step*.

f) After N_T time step modulations, decrease the temperature. The most widely used cooling pattern is geometric and is expressed as follows:

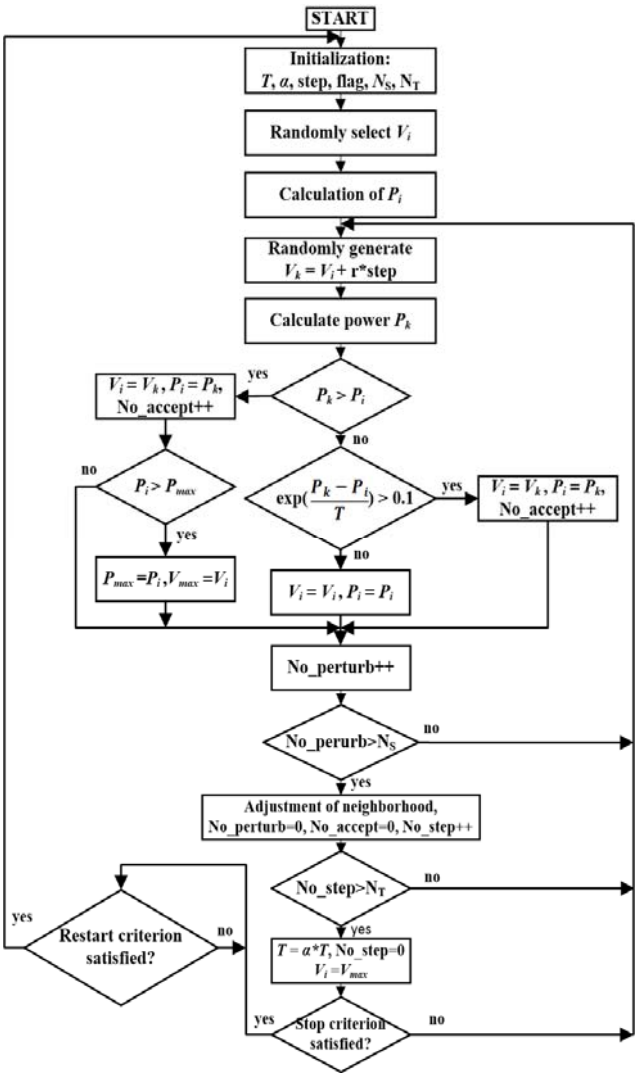

Fig. 5. Flowchart of proposed ESA-based GMPPT algorithm.

$$T_k = \alpha T_{k-1}, \tag{7}$$

where T_k is the temperature of step k, and α is the cooling rate ($0<\alpha<1$). Re-initialization of *No_step*. Let $V_i=V_{max}$.

5. If the algorithm stops, then it immediately terminates voltage perturbation. The system works at its GMPP and prepares for restarting.

IV. Simulation And Test Results

A. Simulation Results

Four simulation cases are provided in MATLAB/Simulink based on a boost circuit with resistive load to evaluate the performance of the proposed ESA-based GMPPT algorithm. Detailed parameters are presented in Table II.

1) Case A (Comparison with Current SA-based GMPPT): In this case, the photovoltaic object is a PV system that consists of three modules. The rating of each module is P_{max}=305W, U_{OC}=44.7V, I_{SC}=8.89A, U_{mpp}=36.2V, and I_{mpp}=8.23A at 1000 W/m^2, 25 °C. The corresponding irradiances are S_1=1000, S_2=800, and S_3=400 W/m^2. At 0.4 s, the irradiance of module 1 and S_1 changes to 400 W/m^2, whereas S_2 and S_3 remain unchanged. Figs. 6(a) and (b) show the static curves of this mismatched PV panel before and after 0.4 s. The peak power drops from 500 W to 352 W, whereas V_{mpp} increases to 105 V from 72 V. Fig. 7 shows the operating voltage and output power.

TABLE II
Simulation Parameters of ESA-based GMPPT Algorithm

Cases	A	B	C	D
U_{OC} (V)	44.7	500	450	500
Initial Temperature(℃)	25	20	20	20
Cooling Rate	0.8	0.8	0.8	0.8
Initial Step(V)	75	150	120	150
Flag	3	3	3	3
N_S	6	6	6	6
N_T	3	3	3	3

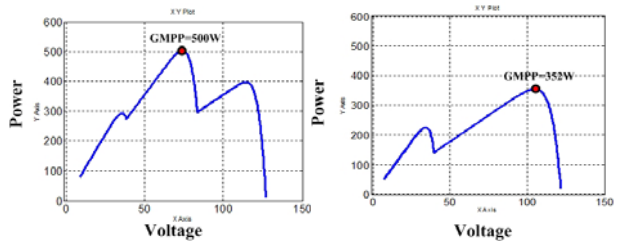

(a) before 0.4 s. (b) after 0.4 s.

Fig. 6. Static curves of shaded PV panel.

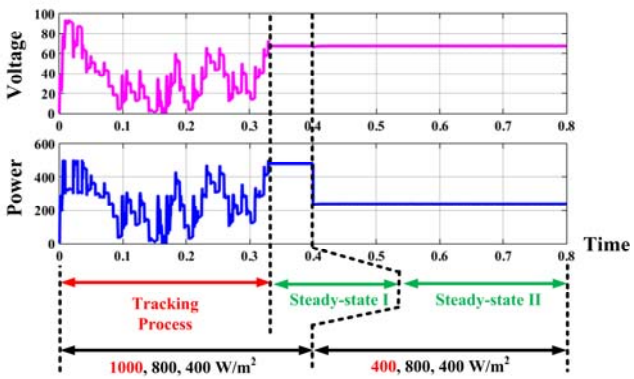

Fig. 7. Output voltage curve and power curve of traditional SA method.

Compared with the current SA-based GMPPT algorithm [12] with the same mismatch case (Fig. 8), three major improvements on restarting capability, stop criterion, and self-adaptive adjustable neighborhood are introduced. Moreover, several advantages can be achieved from the proposed ESA-based GMPPT solution, such as the following:

a) Reboot Capability under Changing Climate: The aforementioned simulation results prove that the ESA-based GMPPT algorithm can detect irradiance changing and activate a new tracking process immediately. Fig. 7 shows that at 0.4 s, the ESA-based GMPPT method can detect irradiance changing and quickly responds to seek a new

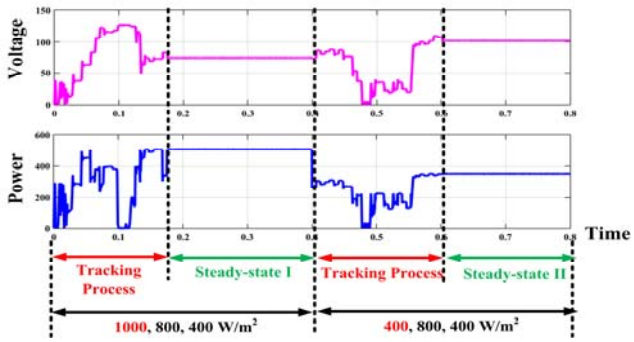

Fig. 8. Output voltage curve and power curve of ESA GMPPT method.

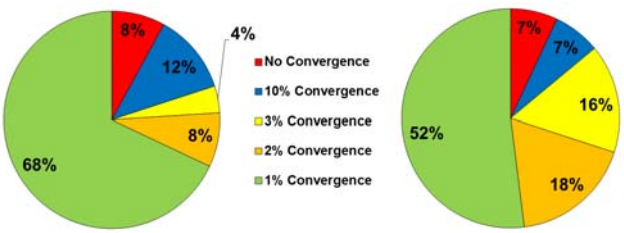

(a) ESA-based method. (b) Traditional SA method.

Fig. 9. Comparison of percentage of accuracy of GMPPT methods.

GMPPT process. Steady state II is achieved after 0.2 s tracking process, as shown in Fig. 7. By contrast, the traditional SA-based GMPPT method cannot restart in this condition, thereby resulting in power loss.

b) Improved Stability and High Precision: The convergence of the traditional SA technique and ESA algorithm are considered and compared in Fig. 9. The 1% convergence indicates the ratio of the number of cases that the operating point converges to within 1% of the voltage value and 1% of the power value of the GMPP. The other indexes are defined on the same basis. The operating point is considered to have not converged precisely if an error of more than 2% convergence occurs. Fig. 9 shows that the proposed ESA algorithm exhibits better performance with respect to its convergence to the GMPP than the traditional SA algorithm, especially in 1% convergence after 50 tests.

c) Rapid Convergence: The proposed ESA solution takes 0.18 s and 0.2 s to reach the GMPP in steady state I and II before and after the irradiance changes, which is much faster and more effective than current solutions, because of the optimized design in flexible self-adaptive neighborhood (0.32 s in Fig. 8).

2) Case B (ESA-based GMPPT in Original PV Array): The photovoltaic object of case B is set to be the original PV array shown in Fig. 2(a). The curve is presented in Fig. 4(a). The reference voltage, operating voltage, and output power of the PV array are provided in Fig. 10, in which only 0.23 s is needed for the ESA algorithm to track the GMPP of the original PV array. Compared with the P–V curve (shown in Fig. 4(a)), the GMPP is precisely tracked. Also, the voltage

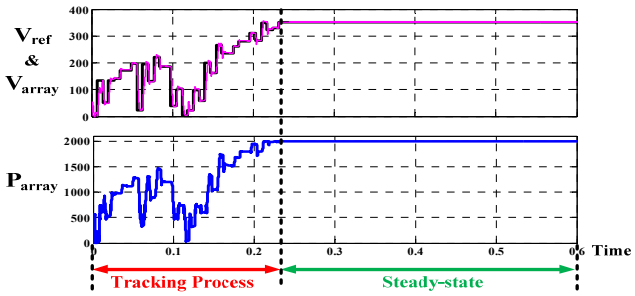

Fig. 10. Output curves of original PV array (Case B).

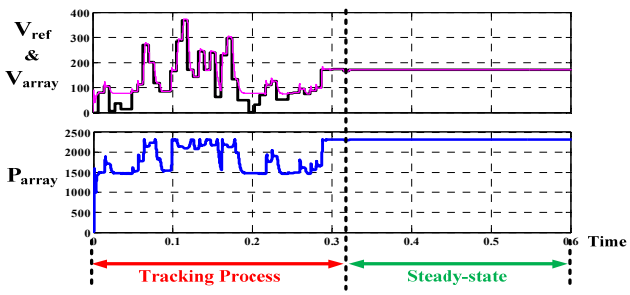

Fig. 11. Output curves of DMPPT PV array (Case C).

perturbation is within a permitted range, with no oscillation in the steady state. The black curve indicates the reference signal voltage and the purple curve indicates the operating voltage of the PV array.

3) Case C (ESA-based GMPPT in DMPPT PV Array): The DMPPT PV array described in Fig. 2(b) with static P–V curve, as shown in Fig. 4(b), is adopted as the photovoltaic object for case C. In this case, the GMPP is quickly and perfectly tracked without deviation or steady-state oscillation. The black curve indicates the reference signal voltage and purple curve indicates the operating voltage of the PV array.

4) Case D (ESA-based GMPPT in Hybrid PV Array): In this case, the ESA-based algorithm is operated on a hybrid PV array whose P–V curve is presented in Fig. 4(c). Similarly, the GMPP is fast and precisely tracked in 0.32 s, without deviation or steady-state oscillation. The black curve indicates the reference signal voltage and purple curve indicates the operating voltage of this PV array.

5) Case E (ESA-based GMPPT in DMPPT PV Array in Normal Mismatch Case): Principally, the DMPPT technique is an effective solution against mismatch without considering additional cost. The output curve of a DMPPT system provides a constant power region in normal mismatch cases. In Fig. 13(a), because of the adoption of DMPPT converters, the output P–V curve can achieve ideal maximum power, suggesting that the individual maximum power of all PV units in different irradiances can be guaranteed. Thus, the ESA algorithm stops seeking process after the operating voltage is inside the constant power region (red region in Fig. 13(a)). The transient and steady-state tracking processes are shown in Fig. 13(b).

As exhibited, the merits of self-reboot capability, increased

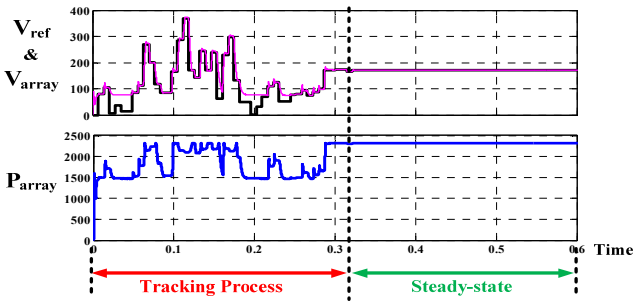

Fig. 12. Output curves of the hybrid PV array (Case D).

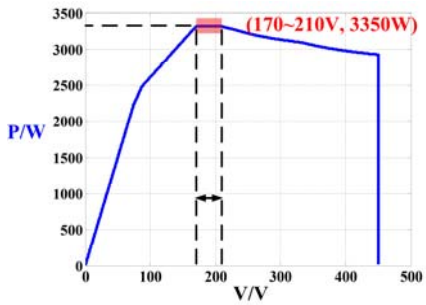

(a) Simulation results.

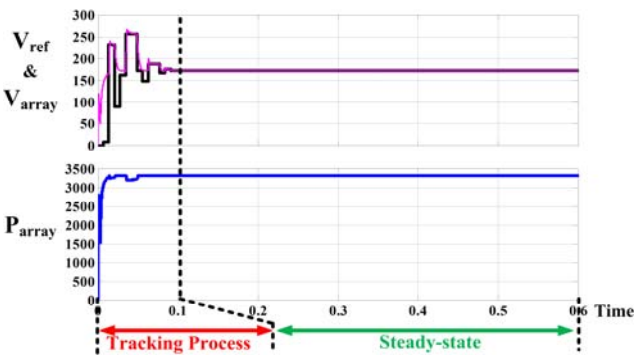

(b) Tracking results in ESA algorithm.

Fig. 13. DMPPT PV array in normal mismatch case (Case E).

TABLE III
EXPERIMENTAL PARAMETERS OF ESA-BASED GMPPT ALGORITHM

Initial Temperature(℃)	10
Cooling Rate	0.8
Initial Step(V)	10
Flag	3
N_S	6
N_T	3

power harvest, and rapid convergence allow the proposal of the ESA solution to provide optimized performance. Moreover, this ESA solution can be applied in the original PV, DMPPT PV, and hybrid PV systems regardless of mismatch. The multi-peak issue that causes mismatch can be solved effectively.

B. Experimental Results

A testbed is built to verify the ESA-based GMPPT algorithm. The characteristics of the PV arrays are

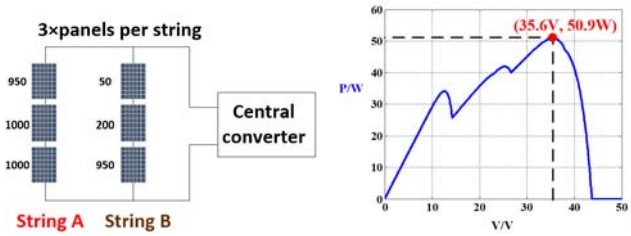

Fig. 14. An original PV array (Case A).

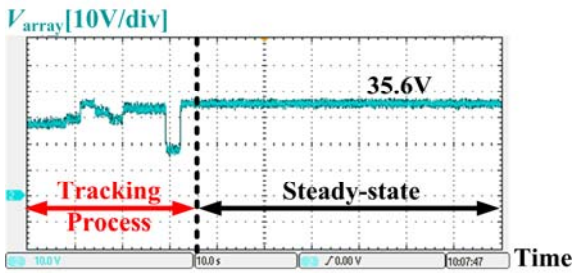

Fig. 15. Operating voltage of original PV array (Case A).

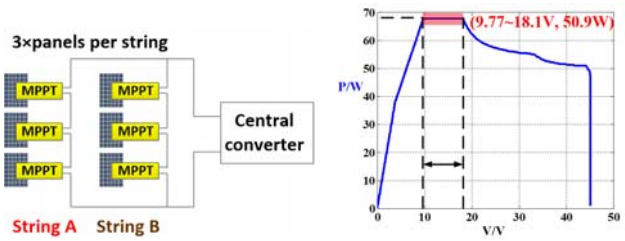

Fig. 16. DMPPT array (Case B).

simulated by a PV simulator (Chroma 62150H-1000S), and the output of the simulator is directly connected to an electronic load via a boost converter. To effectively prove the performance of the algorithm, three cases are experimented and the relative parameters are listed in Table III. A low-power PV output profile is simulated to prove the effectiveness of the ESA algorithm because of the power rating limitation of the adopted boost circuit. Three typical cases are selected to confirm the effectiveness of the ESA solution.

In case A, an original PV system in a mismatch case is considered to verify the ESA solution. The PV array that consists of two PV strings with three PV panel series connected in each string. The output curve of this original PV array is shown in Fig. 14. The number beside the panel represents its irradiance (W/m^2). The P–V curve exhibits three local MPPs, including a GMPP (35.6 V, 50.9 W). The experimental voltage curve is shown in Fig. 15. After several perturbations, the GMPP 35.6 V is tracked without deviation or steady-state oscillation.

In case B, which is similar to case E in the simulation part, the DMPPT PV system works in a normal mismatch case. Two DMPPT strings are parallel connected with each PV panel equipped with an individual MPPT converter, as shown in Fig. 16. The DMPPT array has an ideal constant maximum power region from 9.77 V to 18.1 V, which is represented by

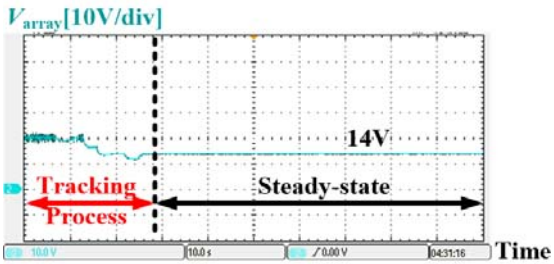

Fig. 17. Operating voltage of DMPPT PV array (Case B).

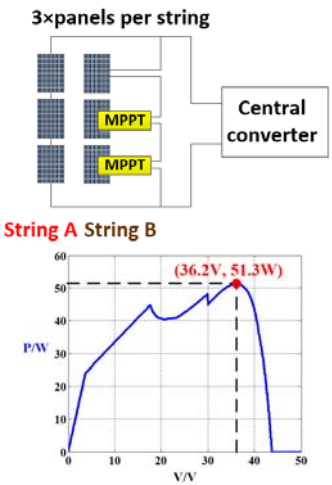

Fig. 18. A hybrid array (Case C).

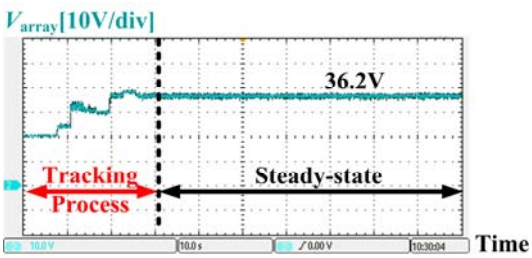

Fig. 19. Voltage curve of hybrid PV array (Case C).

the red region in Fig. 16. The seeking process is shown in Fig. 17. The tracked voltage point is 14 V, which is inside the optimal region and all of the PV units can output its individual maximum power.

In case C, a hybrid PV system with only two panels of the original PV array is equipped with a dedicated MPPT converter, as shown in Fig. 18. In this case, the output PV curve performs multi-peak characteristics, and the ESA algorithm in the second central converter is essential. The experimental voltage curve is presented in Fig. 19. The GMPP 36.2 V is also quickly and precisely tracked without deviation or steady-state oscillation.

The effectiveness of the proposed ESA GMPPT solution has been verified based on various aspects. Moreover, this solution can be applied to different PV systems regardless of the structures. The mismatch issue has also been solved with improved performance in static and transient aspects.

V. Conclusions

Mismatch condition often occurs in large PV generation systems. When mismatch occurs, the P–V characteristic curve of a PV system exhibits multi-peak performance. This paper presents an ESA-based GMPPT control strategy that can be applied for central MPPT control to various PV systems, including original PV array, DMPPT PV array, and hybrid PV array. The proposed strategy not only distinguishes the global MPP among MPPs in the multi-peak P-V curve but also performs fast convergence speed, high tracking accuracy, and anti-mismatch capability. The improvements are validated by MATLAB simulation results, and the feasibility of the proposed ESA-based GMPPT method is verified through experiments.

Acknowledgment

This study was supported by the Natural Science Foundation of China (No. 51407133), the Natural Science Foundation of Shaanxi (No. 2017JQ5049), and the Power Electronics Science and Education Development Program of Delta Environmental and Educational Foundation under Grant No. DREG2015018.

References

[1] B. I. Rani, G. S. Ilango, and C. Nagamani, “Enhanced power generation from PV array under partial shading conditions by shade dispersion using Su Do Ku configuration,” *IEEE Trans. Sustain. Energy*, Vol. 4, No. 3, pp. 594-601, Jul. 2013.

[2] E. V. Paraskevadaki and S. A. Papathanassiou, “Evaluation of MPP voltage and power of mc-Si PV modules in partial shading conditions,” *IEEE Trans. Energy Convers.*, Vol. 26, No. 3, pp. 923-932, Sep. 2011.

[3] S. M. MacAlpine, R. W. Erickson, and M. J. Brandemuehl, “Characterization of power optimizer potential to increase energy capture in photovoltaic systems operating under nonuniform conditions,” *IEEE Trans. Power Electron.*, Vol. 28, No. 6, pp. 2936-2945, Jun. 2013.

[4] Y.-H. Liu, J.-H. Chen, and J.-W. Huang, “A review of maximum power point tracking techniques for use in partially shaded conditions,” *Renewable and Sustainable Energy Reviews*, Vol. 41, pp. 436-453, Jan. 2015.

[5] G. R. Walker and J. C. Pierce, “Photovoltaic DC-DC module integrated converter for novel cascaded and bypass grid connection topologies – Design and optimisation,” in *Power Electronics Specialists Conference*, PESC '06. 37th IEEE, pp. 1-7, 2006.

[6] E. Roman, R. Alonso, P. Ibanez, S. Elorduizapatarietxe, and D. Goitia, “Intelligent PV module for grid-connected PV systems,” *IEEE Trans. Ind. Electron.*, Vol. 53, No. 4, pp. 1066-1073, Jun. 2006.

[7] F. Wang, Z. Fang, F. C. Lee, T. Zhu, and H. Yi, “Analysis of Existence-Judging Criteria for Optimal Power Regions in DMPPT PV Systems,” *IEEE Trans. Energy Convers.*, Vol. 31, No. 4, pp. 1433-1441, Dec. 2016.

[8] M. Kasper, D. Bortis, and J. W. Kolar, “Classification and comparative evaluation of PV panel-integrated DC-DC

converter concepts," *IEEE Trans. Power Electron.*, Vol. 29, No. 5, pp. 2511-2526, May 2014.
[9] F. Wang, F. Zhuo, F. C. Lee, T. Zhu, and H. Yi, "Analysis of Existence-Judging Criteria for Optimal Power Regions in DMPPT PV Systems," *IEEE Trans. Energy Convers.*, Vol. 31, No. 4, pp. 1433-1441, Dec. 2016.
[10] R. Alonso, E. Roman, A. Sanz, V. E. M. Santos, and P. Ibanez, "Analysis of inverter-voltage influence on distributed MPPT architecture performance," *IEEE Trans. Ind. Electron.*, Vol. 59, No. 10, pp. 3900-3907, Oct. 2012.
[11] M. Vitelli, "On the necessity of joint adoption of both Distributed Maximum Power Point Tracking and Central Maximum Power Point Tracking in PV systems," Vol. 22, No. 3, pp. 283-299, Mar. 2014.
[12] S. Lyden and M. E. Haque, "A simulated annealing global maximum power point tracking approach for PV modules under partial shading conditions," *IEEE Trans. Power Electron.*, Vol. 31, No. 6, pp. 4171-4181, Jun. 2016.
[13] C. Zhongsheng, L. Qiang, and F. C. Lee, "Multi-phase smart converter for PV system," in *Applied Power Electronics Conference and Exposition (APEC)*, 2015 IEEE, pp. 1736-1742, 2015.
[14] M. Seyedmahmoudian, R. Rahmani, S. Mekhilef, A. Maung Than Oo, A. Stojcevski, T. K. Soon, and A. S. Ghandhari, "Simulation and hardware implementation of new maximum power point tracking technique for partially shaded PV system using hybrid DEPSO method," *IEEE Trans. Sustain. Energy,* Vol. 6, No. 3, pp. 850-862, Jul. 2015.
[15] P. Manganiello, M. Ricco, G. Petrone, E. Monmasson, and G. Spagnuolo, "Optimization of perturbative PV MPPT methods through online system identification," *IEEE Trans. Ind. Electron.*, Vol. 61, No. 12, pp. 6812-6821, Dec. 2014.
[16] C. Kai, T. Shulin, C. Yuhua, and B. Libing, "An improved MPPT controller for photovoltaic system under partial shading condition," *IEEE Trans. Sustain. Energy*, Vol. 5, No. 3, pp. 978-985, Jul. 2014.
[17] K. Ishaque and Z. Salam, "A deterministic particle swarm optimization maximum power point tracker for photovoltaic system under partial shading condition," *IEEE Trans. Ind. Electron.*, Vol. 60, No. 8, pp. 3195-3206, Aug. 2013.
[18] B. N. Alajmi, K. H. Ahmed, S. J. Finney, and B. W. Williams, "A maximum power point tracking technique for partially shaded photovoltaic systems in microgrids," *IEEE Trans. Ind. Electron.,* Vol. 60, No. 4, pp. 1596-1606, Apr. 2013.
[19] J. Li, Z. Wei, D. Dong, I. Cvetkovic, F. C. Lee, P. Mattavelli, D. Boroyevich, and P. Kong, "R-based MPPT method for smart converter PV system," in *Applied Power Electronics Conference and Exposition (APEC)*, 2012 Twenty-Seventh Annual IEEE, pp. 2072-2079, 2012.
[20] K. Ishaque, Z. Salam, M. Amjad, and S. Mekhilef, "An improved particle swarm optimization (PSO)-based MPPT for PV with reduced steady-state oscillation," *IEEE Trans. Power Electron.*, Vol. 27, No. 8, pp. 3627-3638, Aug. 2012.
[21] H. Patel and V. Agarwal, "Maximum power point tracking scheme for PV systems operating under partially shaded conditions," *IEEE Trans. Ind. Electron.*, Vol. 55, No. 4, pp. 1689-1698, Apr. 2008.
[22] R. Ramaprabha, B. Mathur, A. Ravi, and S. Aventhika, "Modified fibonacci search based MPPT scheme for SPVA under partial shaded conditions," in *2010 3rd International Conference on Emerging Trends in Engineering and Technology*, pp. 379-384, 2010.
[23] H. H. Tumbelaka and M. Miyatake, "Simple integration of three-phase shunt active power filter and photovoltaic generation system with Fibonacci-search-based MPPT," in *2010 IEEE Symposium on Industrial Electronics and Applications (ISIEA)*, pp. 94-99, 2010.
[24] M. Balato, M. Vitelli, N. Femia, G. Petrone, and G. Spagnuolo, "Factors limiting the efficiency of DMPPT in PV applications," in *Clean Electrical Power (ICCEP), 2011 International Conference on*, pp. 604-608, 2011.
[25] W. Feng, W. Xinke, F. C. Lee, W. Zijian, K. Pengju, and Z. Fang, "Analysis of unified output MPPT control in subpanel PV converter system," *IEEE Trans. Power Electron.*, Vol. 29, No. 3, pp. 1275-1284, Mar. 2014.
[26] Y. Fan, F. Zhuo, Y. Yang, F. Wang, T. Zhu, S. Shi, and L. Sun, "An improved simulated annealing maximum power point tracking technique for PV array under partial shading conditions," in *2016 18th European Conference on Power Electronics and Applications (EPE'16 ECCE Europe)*, pp. 1-8, 2016.
[27] Mohamed Arbi Khlifi, "Study and control of photovoltaic water pumping system," *J Electr Eng Technol*, Vol. 11, No. 1, pp. 117-124, Jan. 2016.
[28] D. Thenathayalan, A. Ahmed, B. Choi, J. Park, J. Park "Independent MPP tracking method of hybrid solar-wind power conditioning systems using integrated dual-input single-PWM-cell converter topology," *J Electr Eng Technol*, Vol. 12, No. 2, pp. 790-802, Mar. 2017.

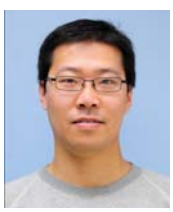

Feng Wang (S'08, M'13) received his B.S., M.S., and Ph.D. degrees in Electrical Engineering from Xi'an Jiaotong University (XJTU), Xi'an, China, in 2005, 2009, and 2013, respectively. From November 2010 to November 2012, he was an exchange Ph.D. student at the Center for Power Electronics Systems at Virginia Polytechnic Institute and State University, Blacksburg, VA. In November 2013, he joined XJTU as a Postdoctoral Fellow. His current research interests include DC/DC conversion and digital control of switched converters, especially in renewable energy generation. He is currently with the State Key Laboratory of Electrical Insulation and Power Equipment, School of Electrical Engineering, XJTU (e-mail: fengwangee@xjtu.edu.cn).

Tianhua Zhu (S'16) received her B.S. degree in Electrical Engineering from Xi'an Jiaotong University (XJTU), Xi'an, China in 2014. She is now pursuing her master's degree in Power Electronics and Renewable Energy Center at XJTU. Her current research interests include maximum-power point-tracking techniques, distributed maximum-power point tracking, and differential power processing. She is with the State Key Laboratory of Electrical Insulation and Power Equipment, School of Electrical Engineering, XJTU (e-mail: zth1222@stu.xjtu.edu.cn).

Fang Zhuo (M'00) was born in Shanghai, China in 1962. He received his B.S. degree in automatic control, and his M.S. and Ph.D. degrees in automation and electrical engineering, from Xi'an Jiaotong University (XJTU), Xi'an, China, in 1984, 1989, and 2001, respectively. He was an associate professor at XJTU in 1996, and a full professor in power electronics and drives in 2004. Then, he worked as a supervisor of Ph.D. students. His research interests include power electronics, power quality, active power filter, reactive power compensation, and inverters for distributed power generation. He is the key finisher of the four projects sponsored by the National Natural Science Foundation of China, and more than 40 projects cooperated with companies from the industry. He received four provincial- and ministerial-level science and technology advancement awards. Moreover, he owns four patents. He is a member of the China Electro Technical Society, Automation Society, and Power Supply Society. He is also the Power Quality Professional Chairman of the Power Supply Society in China.

Hao Yi (S'10–M'14) received his M.S. and Ph.D. degrees in electrical engineering from Xi'an Jiaotong University (XJTU), Xi'an, China in 2010 and 2013, respectively. Since 2013, he has been a faculty member of the School of Electrical Engineering at XJTU. His current research interests include modeling and control of high-power converters, control and power management of microgrids, and power quality improvement.

Yusen Fan received his B.S. degree in electrical engineering from Xi'an Jiaotong University, Xi'an, China in 2016. He is now pursuing his Ph.D. degree in electrical and computer engineering at the University of Maryland (UMD). His research interests include maximum-power point-tracking techniques and algorithms. He is with the Department of Electrical and Computer Engineering, UMD, College Park, Maryland 20742, United States.